An Analytical Model of the Small World Effect in D2D Wireless Networks

MUHAMMAD U. ILYAS [1,2], **(Senior Member, IEEE),**
MUHAMMAD MURTAZA KHAN[1,2]**, (Member, IEEE),**
HAYDER RADHA[3]**, (Fellow, IEEE), AHMED AL-GHAMDI**[1]**,**
AND ASMAA MUNSHI[1]

[1]College of Computer Science and Engineering, University of Jeddah, Jeddah 23890, Saudi Arabia
[2]Department of Electrical Engineering, School of Electrical Engineering and Computer Science, National University of Sciences and Technology, Islamabad 44000, Pakistan
[3]Wireless and Video Communications Lab, Department of Electrical and Computer Engineering, Michigan State University, East Lansing, MI 48824, USA

Corresponding author: Muhammad U. Ilyas (usman.ilyas@seecs.edu.pk)

⋮ **ABSTRACT** Small-world networks are characterized by large clustering coefficients and small characteristic path lengths. These properties are induced by replacing a small fraction of short-range local scale links of a geometric/Euclidean graph with long-range global scale links. Advances in wireless networks allow for cost-efficient addition of secondary long-range wireless interfaces in devices. We derive analytical mean-field solutions for 1) clustering coefficient and 2) characteristic path length of peer-to-peer D2D wireless networks with topologies mimicking small-world networks. In graph-theoretic terms these topologies correspond to geometric graphs of randomly deployed nodes in two-dimensions with range limited shortcuts. The models show that in spite of the fact that links used to create shortcuts are range limited, the network still retains the essential phase difference between characteristic path length and clustering coefficient that is the hallmark of small-world networks when a small fraction of all nodes, as little as $1\% - 5\%$, have range limited shortcut links. We also demonstrate the utility of these models as design tools for determining deployment parameters of small-world wireless sensor networks.

⋮ **INDEX TERMS** D2D, small world networks, wireless networks.

I. INTRODUCTION

The limited range of wireless links naturally imposes geometric or Euclidean graph topologies on wireless networks [1], [2], *i.e.*, only nodes within communication range of each other are connected and capable of communicating directly. Device-to-device (D2D) wireless networks are an application of mesh networks, a class of mobile or stationary multi-hop ad-hoc networks [3] of power constrained nodes. D2D networks appear in many IoT applications that sensing, detection and data gathering applications which impose a many-to-one and/or one-to-many data flows. On the spectrum of randomness of graphs, the ends are occupied by lattice graphs on one end (no randomness) and random graphs on the other (complete randomness). In between these extremes lie small-world networks [4]. Lattice graphs are characterized by strongly connected neighborhoods that imply a high degree of local connectivity and resilience, but rather large diameters. Random graphs [5], on the other hand, are characterized by small diameters (that imply an ability to retrieve and disseminate information quickly) but low degree of local connectivity between nearby nodes. Note that the same topological properties that enable the fast dissemination of information within a network also enable fast information retrieval. Clearly, in the context of D2D wireless networks both, strong connectivity at the local level and small diameters are desirable. Both these properties are defining features of small world networks.

In the past, several attempts were made to leverage the small-world network effect in WSNs [6]–[9]. Guidoni *et al.* [10] proposed on-line models using small-world features to design heterogeneous sensor network topologies. More recently, Jin *et al.* [11] added ZigBee interfaces to cellphones and laptops to reduce their power consumption. Furthermore, Zhang and Li [12] built a similar additional ZigBee wireless interface to augment the WiFi interface of cellphones and laptops with motivations very

---

similar to Jin *et al.* [11]. These models consider the addition of shortcuts, long-range links, to a central sink node that collects or disseminates data to optimize communication. Shortcut links in graphs are agnostic with regards to any sense of distance between the nodes they connect, *i.e.*, in the current context, shortcuts are not range limited.

Watts [4] and [13] developed a host of analytical models for one-dimensional lattice graphs, connected caveman graphs and Moore graphs. However, to the authors' best knowledge there are no analytical models of two-dimensional Euclidean graphs with range-limited shortcuts that are typical of D2D wireless networks of devices equipped with short-range and long-range RF interfaces. This paper is a first attempt at deriving analytical models for the clustering coefficient and characteristic path length of D2D wireless networks whose topologies are augmented by long-range RF interfaces, that make up a small fraction of the total number of links, and whose range is restricted by physical limitations due to radio propagation effects. Results show that in spite of the fact that shortcuts in D2D networks are range-limited, the phase difference between drop in clustering coefficient and characteristic path length still occurs with increasing number of shortcuts, which is the defining characteristic of small world networks. Only $1 - 5\%$ of nodes need to activate long-range links at a time in order for the network to become a small-world network, even when the shortcuts are range-limited. The model is able to provide guidance as to what proportion of more capable devices should be introduced into such a mix in order to achieve the desired small-world effect.

Paper Organization: The remaining paper is organized as follows. Section II provides a brief background of small-world networks, their properties and their relationship with Euclidean and random graphs. Section III describes different system models for building D2D wireless networks with small world topologies and provides a literature review of prior developed methods. Section IV uses mean field analysis to derive generalized expressions of clustering coefficient and characteristic path length that are used to model small-world networks based on any of the system models in Section III. Section V evaluates the model for different ranges of parameters. Section VI concludes the paper.

II. BACKGROUND: SMALL WORLD NETWORKS

Small-world networks were first discovered by Milgram in social networks in [14]. Watts [4], [13] analyzed social networks, which included a collaboration network of actors and a collaboration network of mathematicians, to verify Milgram's idea of six degrees of separation. More recently, Whoriskey [15] empirically verified the six degrees of separation in social networks using a much larger data set of instant messaging traffic of Microsoft's Windows Live Messenger. Since Milgram's original experiment, several other works have analyzed networks in natural and man-made systems to discover that their topologies are in fact small-world graphs.

Latora and Marchiori [16] and Watts [13] analyzed the neural network of the C.elegans worm. Montoya and SolÉ [17] studied food webs in nature. Moore and Newman [18], [19] studied the transmission of infectious diseases in populations with small-world connectivity. Studies of transportation networks include Latora and Marchiori [16], [20] on the Boston subway network and Sen *et al.* [21] on the Indian railroad network. Small-world analysis of communication networks include Adamic's [22] on the World Wide Web. I Cancho and Sole [23] studied the lexical networks of human languages and determined them to be small-worlds. More relevant to our work are studies on creating small-world topologies in wireless networks by various means. Wan *et al.* [8], Cavalcanti *et al.* [24] and Costa and Barros [25] showed that selectively equipping a small fraction of nodes in a WSN with two radios (short-range IEEE 802.15.4 and long-range IEEE 802.11b) induces a small-world topology. Hubaux *et al.* [26] and Dimitar *et al.* [27] proposed a small-world application layer for ad hoc networks similar to logical links in peer-to-peer networks. Dixit *et al.* [28] analyzed the topology of cellular wireless networks. Helmy [29], [30] proposed mobility assisted wireless networks to create shortcuts that mimic random links. Sharma and Mazumdar [6] made selected use of wired links to create shortcuts.

Among prior models of small-world networks are Watts' [4] models for the clustering coefficient and characteristic path length of 1-dimensional (circular) lattice graph, connected caveman graphs and Moore graphs. Newman *et al.* [31] found a mean-field solution of the small-world network model for 1-dimensional lattices. Amaral *et al.* [32] studied the statistical properties of classes of small-world networks using a taxonomy based on the form of degree distribution of nodes. Inaltekin *et al.* [33] presented the octopus model for studying small-world networks. Advances in wireless networking have enabled the addition of longer-range wireless links, called *shortcuts* or *global scale links*, to a network by various means (at a cost). In this paper, we derive analytical expressions for two defining properties of small-world networks, *i.e.*, the clustering coefficient C and characteristic path length L of geometric graphs in a 2-dimensional plane with a number of range limited shortcut links. Let $G(V, E)$ denote a graph consisting of a set of N vertexes $V = \{v_1, v_2, v_3, \ldots, v_N\}$ and a set E of M edges consisting of all edges, where $e_{i,j}$ denotes an undirected edge from v_i to v_j.

A. CHARACTERISTIC PATH LENGTH

Characteristic path length is defined as the average length of geodesic paths between all pairs of nodes. For a graph G, the characteristic path length L is defined as the number of edges in the geodesic path between two vertexes, averaged over all pairs of vertexes. If $L_{i,j}$ is the number of edges on the geodesic path from v_i to v_j, then,

$$L = \frac{\sum_{i=1}^{N} \sum_{j=1}^{N} L_{i,j}}{N(N-1)} \quad (1)$$

B. CLUSTERING COEFFICIENT

The clustering coefficient is a measure of cliquishness, the degree to which vertexes in a graph coalesce into tight groups. For a graph G, the clustering coefficient $C(G)$ is defined as follows: Suppose a vertex v has k_v number of neighbors, then the maximum possible size of the set of undirected edges between v and all its neighbors is $\frac{k_v(k_v+1)}{2}$. Then the clustering coefficient C_v is the fraction of these edges that actually exist in E. The clustering coefficient of the graph is then defined as the average C_v over all vertexes V, as in Equ. 2.

$$C = \frac{\sum_{v=1}^{N} C_v N}{N} \qquad (2)$$

The above definitions of characteristic path length and clustering coefficient are easily extended to directed and weighted graphs.

C. SMALL-WORLD, GEOMETRIC AND RANDOM GRAPHS

We will be using the terms graph and network and the terms node and vertex interchangeably. Geometric graphs (see Fig. 1a), have both large L and C by virtue of their strong local connectivity. Random graphs (see Fig. 1b) are the other extreme and are characterized by both small L and C. Small world networks (see Fig. 1c) have small L but large C.
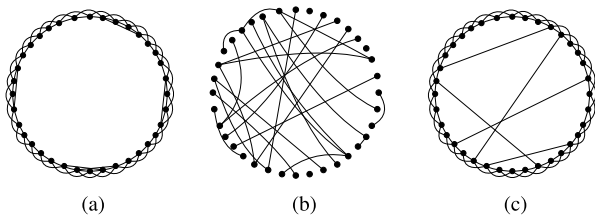

FIGURE 1. Illustrated examples for three different classes of graphs; a) Geometric graph, b) random graph, and c) small world graph.

There are several construction methods for small-world networks. Among the simplest to understand is the β-model described by Watts [4]. A small-world network can be constructed from a lattice or geometric graph by rewiring one end of every edge to a randomly selected node with probability β. If $\beta = 0$, the graph remains a lattice / geometric graph, while $\beta = 1$ yields a random graph. Watts and Strogatz [34], Newman and Watts [35], Pandit and Amritkar [36] and Watts [4] repeatedly demonstrated $\beta = 0.01 - 0.05 \approx \mathcal{O}\left(\frac{1}{N}\right)$ as a typical range of values for constructing small-world networks, which means only a very small fraction of links has to be rewired. Hence, on the scale of randomness where lattice / geometric graphs lie on one extreme and random graphs on the other, small-world graphs fall in between the two, but closer to the former than the latter.

In the context of D2D networks, the property of random graphs to propagate information quickly means that nodes can relay data quickly. The property of Euclidean graphs to have high C and strong local connectivity produces a stable network structure difficult to partition. It also enables the formation of clusters which facilitates collaboration among groups of nodes. Thus, the D2D applications demands the best of Euclidean and random graphs.

III. SMALL WORLD TOPOLOGY CONSTRUCTION METHODS FOR WIRELESS NETWORKS

There are several approaches to realize shortcuts in D2D wireless networks with the intent of creating a small-world topology. We conducted a survey of practical techniques.

A. HYBRID SENSOR NETWORK

Sharma and Mazumdar [6] and Chitradurga and Helmy [7] proposed the judicious use of wired links between a small subset of nodes in a WSN. The resultant network is not a pure wireless network and is called a *hybrid network*. The graph topology of hybrid networks uses range limited links for shortcuts instead of truly random links. From a practical perspective, the wired shortcuts limit the possible deployment scenarios.

B. MULTI-RADIO NETWORK

Wan *et al.* [8] was the first to propose the use of multi-radio nodes as a mean for building small worlds, with the objective of easing congestion in the primary network consisting of ubiquitous low-rate links. The multi-radio node architecture has the disadvantage that it requires a heterogeneous mix of motes / nodes. The links of the long range radio interface serve as small world shortcut links. The implementations used in [8], [11], and [12] use IEEE 802.15.4 [37] in conjunction with the IEEE 802.11b [38] network interface. The significantly higher power consumption of IEEE 802.11b is a disadvantage in power constrained wireless networks.

C. RECEIVER SIDE COOPERATION

The third solution is dubbed the 'Poor man's SIMO system' (PMSS). Ilyas *et al.* [39] describe the gPMSS and how three well-known diversity combination techniques are adopted for use in a network of off-the-shelf IEEE 802.15.4 devices. The diversity combination techniques are derivatives of diversity combining methods for analog signals (see [40]). Simply put, the purposes of diversity combining are twofold; a) Select an error-free version of a received transmission from among multiple received versions or, b) if the first goal is not achievable, obtain another version of the transmission, with no errors or fewer errors than any of the individual received versions. It uses receiver side diversity combining techniques in a network of commercial-off-the-shelf components. Its principal strength over hybrid sensor networks and multi-radio networks is that it circumvents the need for customized or reconfigured hardware. Instead, it relies on receiver side cooperation between a group of motes to form a SIMO system. Ilyas *et al.* [39] describe an efficient PMSS protocol through which information sharing between motes is enabled. This way cooperation reduces losses and retransmissions while increasing throughput and channel utilization.
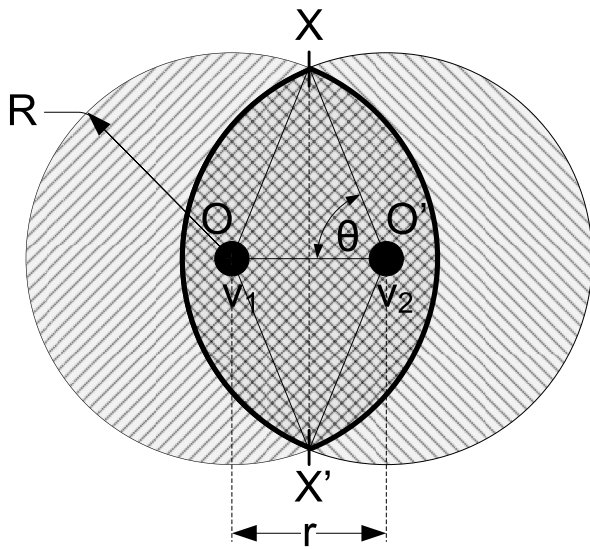
FIGURE 2. Overlapping communication regions of two communicating nodes in a WSN.

In conclusion of this survey, it should be understood that as diverse as these different implementations of small-world networks in wireless networks may be, the analytical model proposed here can be parametrized accordingly.

D. MODEL ASSUMPTIONS

The model proposed in this paper is very flexible to accommodate many kinds of wireless network deployments. It allows for different node deployment densities, coverage areas, communication ranges for short and long range communication links, mixing ratios of short and long range communication nodes. No assumption is made about the mechanism used to create long range communication links or the shape of the hull of the area covered by the sensors. The model makes the assumption that a network forms a single connected component.

In addition, we assume nodes to be randomly distributed according to a Poisson point process, *i.e.*, we do not assume a regular graph structure for the underlying communication network as in [41]–[44].

IV. MEAN FIELD ANALYSIS OF SMALL WORLD WIRELESS NETWORKS

A. CLUSTERING COEFFICIENT

Nodes are distributed according to a 2-dimensional uniform distribution with mean ρ points (nodes) per unit area. Let there be two nodes v_1 and v_2 capable of communicating with nodes within range R_1 and R_2, respectively. For simplicity's sake we will take $R_1 = R_2 = R$. Two nodes will be able to communicate with each other only if they are separated by a distance $r < R$. If the two nodes are separated by a distance $r < R$, then communication coverage regions of nodes v_1 and v_2 will overlap, as depicted by the crisscross pattern region in the simplified model's overlapping region in Fig. 2. Let Δ

denote the size of the overlapping communication coverage regions. Then Δ is computed by adding the areas of sectors XOX' and $XO'X'$ and subtracting the areas of triangles XOX' and $XO'X'$ (because they have been added twice during the addition of both sectors). The resulting expression for Δ is shown in Equ. (3).

$$\Delta(\theta, R) = 2 \cdot \frac{2\theta}{2\pi} \pi R^2 - 2 \cdot R\sin\theta \cdot R\cos\theta$$
$$= 2\theta R^2 - R^2 \sin 2\theta \qquad (3)$$

Here θ is the central angle $\angle XOO'$(congruent to $\angle X'OO'$, $\angle XO'O$ and $\angle X'O'O$) in Fig. 2. We can express θ as a function of r.

$$\theta(r, R) = \arccos \frac{r/2}{R} \qquad (4)$$

Substituting the expression for θ in Equ. (4) back into Equ. (3) gives us Δ as a function of r.

$$\Delta(r, R) = 2R^2\theta(r, R) - 2R^2\sqrt{1 - \frac{r^2}{4R^2}} \cdot \frac{r}{2R}$$
$$= 2R^2 \arccos\left(\frac{r}{2R}\right) - rR\sqrt{1 - \frac{r^2}{4R^2}} \qquad (5)$$

As we already described, for the network topology to be a small world, some nodes have to provide *shortcuts* or *global scale links* to other nodes. These nodes will be referred to as *shortcut nodes* or *global scale nodes*. The number of local nodes and global nodes are denoted by N_{local} and N_{global}, respectively. In literature, the sub-graph formed by global scale nodes is also referred to as a network's substrate [4]. The remaining nodes that are not part of the substrate are called *local scale nodes*. The ratio of the maximum communication range of global scale link to that of a local scale link is called the scaling factor ξ.

Now, let ρ denote the average node density with which nodes occupy the covered region. The cooperative communication model for small world WSNs in Section III-C for the implementation of shortcuts in a wireless network requires multiple nodes to function as a single receiver. Depending on how many nodes are collapsed into a single node (see [39] for details), this will reduce the effective node density from ρ to a lower value ρ'. Let n_c denote the average number of nodes that combine to function as a global scale node. This reduces the node density in the equivalent small world graph (spread over area A) to ρ' which relates to ρ according to Equ. (6).

$$\rho' = \rho - \frac{N_{global}(n_c - 1)}{A} \qquad (6)$$

Note that when shortcut links are implemented in hybrid networks (Subsection III-A) and multi-radio networks (Subsection III-B), the node density in the small world graph remains unchanged, *i.e.*, $n_c = 1$ which implies $\rho' = \rho$. Then, $\Delta(r, R)\rho'$ denotes the number of edges a node (v_1) at a distance r away from a reference node (v_2) has with the set of nodes that can also communicate with the reference node.

Let $\Gamma(v)$ denote the neighborhood of a vertex $v \in V$, where V is the set of all vertexes in the graph G of the wireless network's topology. We treat the entire region covered by nodes as a continuous, homogeneous "sea" of sensors populated with a uniform density of ρ' nodes per unit area. Then the total number of edges d in the neighborhood of vertex v can be computed by integrating $\Delta(r, R)\rho'$ with respect to r over the interval $[0, R]$, the radius of the communication range;

Let $d(\Gamma(v))$ denote the number of edges in the neighborhood $\Gamma(v)$ of a node v. The exact derivation of the expression for $d(\Gamma(v))$ in Equ. (7) is provided as Lemma 1.

$$d(\Gamma(v)) = \pi \rho'^2 R^3 (3.574R - \sqrt{3}) \qquad (7)$$

Let $D(\Gamma(v))$ denote the number of edges in the completely connected graph of node v and its neighborhood $\Gamma(v)$.

$$\begin{aligned} D(\Gamma(v)) &= \pi \rho' R^2 \times \pi \rho' R^2 \\ &= \pi^2 \rho'^2 R^4 \end{aligned} \qquad (8)$$

The clustering coefficient is defined as the expected value of the ratio of the number of links in a node's neighborhood to the number of links in a complete graph of its neighborhood. This can also be defined in terms of previously computed values as;

$$C(G) = E_V \left[\frac{d(\Gamma(v))}{D(\Gamma(v))} \right] \qquad (9)$$

For a node that is part of the sea of nodes communicating over local scale links only, the clustering coefficient C_{local} is defined as,

$$C_{local} = \frac{d(\Gamma(v))}{D(\Gamma(v))} = \frac{3.574R - \sqrt{3}}{\pi R} \qquad (10)$$

Hence, C_{local} grows $\mathcal{O}\left(\frac{1}{R}\right)$ with respect to R. For a global scale node that is part of the substrate communicating over local as well as global scale links, we compute the clustering coefficient C_{global} as,

$$C_{global} = \frac{d(\Gamma(v)) + k_{global}}{D(\Gamma(v)) + k_{global}(\rho'\pi R^2) + (k_{global} - 1)!} \qquad (11)$$

Here, k_{global} is the average degree of nodes in the substrate with other nodes in the substrate. The numerator term in Equ. (11) is the average number of links in the neighborhood of a global scale node, which equals the number of links expected for a local scale node in its place plus the global scale links to other nodes part of the substrate. The denominator term is the average number of links possible between all nodes in the neighborhood of a global node. Note that in doing so, we assumed that $\xi \geq 2$, *i.e.*, none of the neighboring global scale nodes is within communication range of any of the local scale neighbor nodes under consideration. The function for C_{global} grows as $\mathcal{O}\left(\frac{1}{k_{global}!}\right)$. It must be noted here that in the computation of C_{local} and C_{global} we have ignored border effects. In effect, we have assumed that nodes are located on a torus. To obtain the clustering coefficient of the network, C_{local} and C_{global}, are combined in the ratios

in which local and global scale nodes appear. If we define $\mu = \frac{N_{global}}{N_{global} + N_{local}}$, then C is obtained by Equ. 12.

$$C = \mu C_{global} + (1 - \mu)C_{local} \qquad (12)$$

B. CHARACTERISTIC PATH LENGTH

The *characteristic path length* of a graph is defined as the average length of all geodesic paths (measured in hops). In a graph $G(V, E)$ the characteristic path length L is defined as the average of geodesic path lengths $l(v_i, v_j)$ between all connected pairs of vertexes $v_i, v_j \in V$ and $v_i \neq v_j$. Like the clustering coefficient, the characteristic path length is also a function of the number of nodes with global scale links. Since the global scale links are range-limited, and since global scale nodes have to be placed within communication range of one another to be useful, the area covered by them is also limited. The region of the wireless network that is serviced by global scale nodes may even be fragmented into many different patches. Fig. 3 shows a model of a D2D wireless network. For analytical ease, the shape of the region covered by all nodes of the network is approximated by a circle of radius $\sqrt{\frac{A}{\pi}}$ and center O. The region covered by global scale nodes is approximated by a circle of radius $\sqrt{\frac{A_g}{\pi}} < \sqrt{\frac{A}{\pi}}$, also with center O. The difference between coverage areas of the entire wireless network and coverage area of global scale nodes alone is a result of the constraint imposed by a) the limited range of shortcuts and b) the *global vertex degree* (the number of shortcut links incident on a substrate node). Fig. 3 also shows a node at a distance x from O. For the node in the figure, $x > \sqrt{\frac{A_g}{\pi}}$ and the region covered by the nodes can be divided into three separate regions, numbered 1, 2 and 3
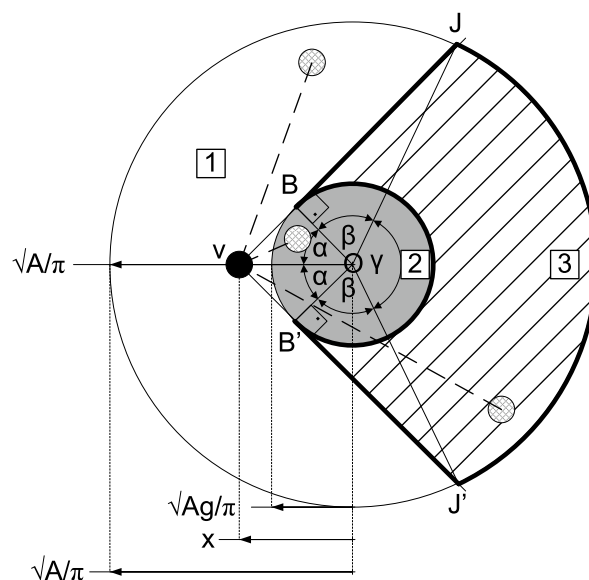

FIGURE 3. Geometry of wireless network deployment and regions within it with respect to an individual sensor v_i.

in Fig. 3. These regions are defined relative to every node v. Region 1 consists of all nodes that are reachable from v without having to traverse any global scale links. In Fig. 3, for node v at distance x from center O, region 1 corresponds to the unshaded white region. Region 2 is the area of size A_g occupied by global scale nodes and is colored solid gray. Region 3 is the region occupied exclusively by sensors with local scale links but which is reachable (by a shortest path) only after traversing region 2. In Fig. 3, region 3 is identified by shading and its area is denoted by $S(x)$. Assuming the deployment of nodes is sufficiently dense, we approximate the geodesic path from one node to another by a straight line between them. To proceed we define three central angles $\alpha = \frac{1}{2}\angle BOB'$, $\beta = \angle BOJ = \angle B'OJ'$ and $\gamma = \angle JOJ'$, where $2(\alpha + \beta) + \gamma = 2\pi$. Since α and γ are functions of x we will be denoting them by $\alpha(x)$ and $\gamma(x)$.

$$\alpha(x) = \arccos \frac{\sqrt{\frac{A_g}{\pi}}}{x} \tag{13}$$

$$\beta = \arccos \frac{\sqrt{\frac{A_g}{\pi}}}{\sqrt{A}} \tag{14}$$

$$\gamma(x) = 2\pi - 2\alpha(x) - 2\beta$$
$$= 2\left(\pi - \arccos \frac{\sqrt{\frac{A_g}{\pi}}}{x} - \arccos \frac{\sqrt{\frac{A_g}{\pi}}}{\sqrt{A}}\right) \tag{15}$$

The area of the region in Fig. 3 labeled region 3 is given in Equ. (16) (see Lemma 2 in the appendix).

$$S(x) = \frac{4\sqrt{AA_g}\sin\beta + A(\pi - \alpha(x) - \beta) - (2\beta + \gamma)A_g}{2\pi} \tag{16}$$

Characteristic path length is denoted by L. It is the average length (in hops) of all geodesic paths from every node $v_i \in V$ to every other node $v_j \in V$. L_{local} is the average number of hops contributed to geodesic paths by local scale links, while L_{global} is the average number of hops contributed to geodesic paths by global scale links. Then L can be expressed as Equ. (17).

$$L = L_{local} + L_{global} \tag{17}$$

Based on the three regions of the wireless network in Fig. 3, geodesic paths are classified into one of four different types.

- **Type 1:** Geodesic paths that originate from and terminate at nodes in region 1 (outside the region covered by the substrate). Type 1 paths consist of local scale links only.
- **Type 2:** Geodesic paths that originate from a node in region 1 and terminate at a node in region 2.
- **Type 3:** Geodesic paths that originate from a node in region 1 and terminate at a node in region 3. Such paths pass through region 2.
- **Type 4:** Geodesic paths that originate from and terminate at nodes in region 2.

We compute L_{local} (L_{global}) in Equ. (18) (Equ. (19)) as the sum of $L_{local}(i)$ ($L_{global}(i)$), the contributions of local (global)

scale links to type i paths, weighted by the normalized frequency of occurrence of type i paths.

$$L_{local} = \frac{1}{R}\sum_{i=1}^{4} L_{local}(i) \tag{18}$$

$$L_{global} = \frac{1}{\xi R}\sum_{i=1}^{4} L_{global}(i) \tag{19}$$

For a node v in region 1 at $x > \sqrt{\frac{A_g}{\pi}}$ distance from O, let $l_{local}^{(1)}(x)$ denote the average spatial distance on type 1 paths traversed over local scale links. Then, for a particular node, the size of region 1 is $A - A_g - S(x)$. Since the deployment of nodes is in two dimensions, we approximate the size of the region traversed by these paths by the square root of its area, $\sqrt{A - A_g - S(x)}$. Although region 1 is irregularly shaped, we approximate the average of all-pairs shortest paths of nodes in region 1 by an approximation of the 'radius' of region 1, *i.e.* half of the square root of the area. This is denoted by $l_{local}^{(1)}(x)$ and is approximated as by Equ. (20).

$$l_{local}^{(1)}(x) = \frac{1}{2}\sqrt{A - A_g - S(x)} \tag{20}$$

A node v at distance $x > \sqrt{\frac{A_g}{\pi}}$ from O has shortest paths of average length $\rho l_{local}^{(1)}(x)$ to other nodes in region 1. To obtain $L_{local}(1)$, we integrate $l_{local}^{(1)}(x)$ over all nodes in region 1, *i.e.* the region of deployment of the wireless network that lies outside the substrate, which is all nodes for which x lies in the range $\sqrt{\frac{A_g}{\pi}} < x < \sqrt{\frac{A}{\pi}}$. The term $\rho 2\pi x$ represents the number of nodes at a distance x from the center of the sensor region and is integrated over x. The remaining third term in Equ. (21) is $\rho(A - A_g - S(x))$ and represents the number of nodes to which a node v at distance x can have a path.

$$L_{local}(1) = \frac{1}{(\rho'A)^2}\int_{\sqrt{\frac{A_g}{\pi}}}^{\sqrt{\frac{A}{\pi}}} \rho 2\pi x \cdot \rho\left(A - A_g - S(x)\right)$$
$$\times l_{local}^{(1)}(x)dx \tag{21}$$

Since the paths from v to other nodes in region 1 do not traverse region 2, no global scale links are used. Hence $L_{global}(1)$, the component of global scale links in paths to nodes in region 1 is 0, as in Equ. (22).

$$L_{global}(1) = 0 \tag{22}$$

For a node v in region 1 at $x > \sqrt{\frac{A_g}{\pi}}$ distance from O, let $l_{local}^{(2)}(x)$ denote the average spatial distance on type 2 paths traversed over local scale links. It is approximated by the mean of the shortest $(x - \sqrt{\frac{A_g}{\pi}})$ and longest distances (from node v to point B) from v to a node in region 2, *i.e.* $\frac{1}{2}(x - \sqrt{\frac{A_g}{\pi}} + x\sin\alpha(x))$. To include paths from nodes in region 2 back to node v, we multiply this term by a factor of 2. This is

approximated by $l_{local}^{(2)}(x)$ in Equ. (23).

$$l_{local}^{(2)}(x) = \frac{(x - \sqrt{\frac{A_g}{\pi}} + x \sin \alpha(x))}{2} \quad (23)$$

$L_{local}(2)$ (Equ. (18)) is the component of L_{local} contributed by node v's type 2 paths, *i.e.*, to other nodes in region 2. A node v at distance $x > \sqrt{\frac{A_g}{\pi}}$ from O has $\rho'' A_g$ paths to other nodes in region 2. To obtain $L_{local}(2)$, we integrate this term over all circumferences of radii x in the range $\sqrt{\frac{A_g}{\pi}} < x < \sqrt{\frac{A}{\pi}}$. This is shown in Equ. (24).

$$L_{local}(2) = \frac{1}{(\rho'A)^2} \int_{\sqrt{\frac{A_g}{\pi}}}^{\sqrt{\frac{A}{\pi}}} \rho 2\pi x \cdot \rho'' A_g l_{local}^{(2)}(x) dx \quad (24)$$

Here ρ'' is the node density of nodes in region 2 only, excluding region 1 and region 3.

$$\rho'' = \rho - \frac{N_{global}(n_c - 1)}{Ag} \quad (25)$$

The length of global scale paths from v to sensors in region 2 is approximated like in Equ. (26).

$$l_{global}^{(2)}(x) = \sqrt{\frac{A_g}{\pi}} \quad (26)$$

Equ. (27) weighs this by the number of paths from all nodes v outside of region 2 to all $\rho'' A_g$ sensors inside region 2 (and vice versa) relative to the number of paths between all pairs of nodes, *i.e.* $(\rho'A)^2$.

$$\begin{aligned} L_{global}(2) &= \frac{1}{(\rho'A)^2} \int_{\sqrt{\frac{A_g}{\pi}}}^{\sqrt{\frac{A}{\pi}}} \rho 2\pi x \rho'' A_g \sqrt{\frac{A_g}{\pi}} dx \\ &= \frac{\rho \rho'' A_g^{3/2}(A - A_g)}{\sqrt{\pi}(\rho'A)^2} \end{aligned} \quad (27)$$

For a node v in region 1 at $x > \sqrt{\frac{A_g}{\pi}}$ distance from O, let $l_{local}^{(3)}(x)$ denote the average spatial distance on type 3 paths traversed over local scale links. It is approximated by Equ. (28). The first term $l_{local}^{(3)}(x)$ represents the distance traversed by a path over local links before entering the region 2 of the wireless network which is serviced by the substrate, and the second term represents the distance traversed over local scale links after exiting region 2.

$$\begin{aligned} l_{local}^{(3)}(x) &= l_{local}^{(2)}(x) + \frac{\sqrt{\frac{A}{\pi}} - \sqrt{\frac{A_g}{\pi}}}{2} \\ &= \frac{1}{2} \left(x + \sqrt{\frac{A}{\pi}} - 2\sqrt{\frac{A_g}{\pi}} + x \sin \alpha(x) \right) \end{aligned} \quad (28)$$

A node v at distance $x > \sqrt{\frac{A_g}{\pi}}$ from O has $\rho S(x)$ paths to other nodes in region 3. To obtain $L_{local}(3)$, we integrate $l_{local}^{(3)}(x)$ over all circumferences of radii x in the range $\sqrt{\frac{A_g}{\pi}} < x < \sqrt{\frac{A}{\pi}}$. This is shown in Equ. (29).

$$L_{local}(3) = \frac{1}{(\rho'A)^2} \int_{\sqrt{\frac{A_g}{\pi}}}^{\sqrt{\frac{A}{\pi}}} \rho 2\pi x \cdot \rho S(x) l_{local}^{(3)}(x) dx \quad (29)$$

For $L_{global}(3)$ in Equ. (30), we approximate the length of global scale links by the diameter of region 2, $2\sqrt{\frac{A_g}{\pi}}$, and weight it by the total number of paths from all nodes v in region 3, which is $\rho S_d(x)$.

$$L_{global}(3) = \frac{1}{(\rho'A)^2} \int_{\sqrt{\frac{A_g}{\pi}}}^{\sqrt{\frac{A}{\pi}}} \rho 2\pi x \cdot \rho S(x) 2\sqrt{\frac{A_g}{\pi}} dx \quad (30)$$

Finally, for a node v in region 2 at distance $x < \sqrt{\frac{A_g}{\pi}}$ from O, let $l_{local}^{(4)}$ denote the average spatial distance on type 4 paths traversed over local scale links. We assume that on average, a node v in region 2 communicating with another node in region 2 will route (over local links) to a nearby node with global scale links. Once traffic has reached the vicinity of the destination node, traffic is routed over local scale links to the destination. Let h_{max} denote the maximum distance of a node in region 2 to its closest global scale node, as expressed in Equ. (31).

$$h_{max} = \arg\max_h \sum_{h=1} \rho' \left[(hR)^2 - ((h-1)R)^2 \right] \le \frac{\pi A_g}{N_{global}} \quad (31)$$

Since equidistant nodes form concentric bands around global scale nodes, the probability mass function $p_H(h)$ of the hop distance H is modeled by Equ. (32).

$$p_H(h) = \frac{\pi(hR)^2 - \pi((h-1)R)^2}{\pi(h_{max}R)^2} = \frac{2h-1}{h_{max}^2} \quad (32)$$

Then $l_{local}^{(4)}$ is approximated by the expected value of H as in Equ. (33).

$$l_{local}^{(4)} = E_H[h] = \sum_{h=1}^{h_{max}} h \frac{2h-1}{h_{max}^2} \quad (33)$$

A node v at distance $x < \sqrt{\frac{A_g}{\pi}}$ from O, within region 2, has $\rho'' A_g$ paths to other nodes in region 2. $L_{local}(4)$ in Equ. (33) is the weighted, average contribution of paths from nodes in region 2 to other nodes in region 2 over local scale links. A factor of 2 is added in the term because a path may go over local scale links to i) reach the closest global scale node on the way to a destination, and ii) from the last global scale node on the path and to the destination node. Similarly, $L_{global}(4)$ in Equ. (34) is the weighted, average contribution of paths from nodes in region 2 to other nodes in region 2 over global scale links.

$$L_{local}(4) = \frac{2(\rho'' A_g)^2}{(\rho'A)^2} l_{local}^{(4)} \quad (34)$$

$$L_{global}(4) = \frac{(\rho'' A_g)^2}{(\rho'A)^2} \sqrt{\frac{A_g}{\pi}} \quad (35)$$

Now we can back substitute Equ. 21, Equ. 24, Equ. 29 and Equ. 34 into Equ. (18) to obtain L_{local}. Similarly, Equ. 22, Equ. 27, Equ. 30 and Equ. 35 are put back into Equ. 19 to obtain L_{global}. Equ. 18 and Equ. 19 are substituted into Equ. 17 to obtain the characteristic path length L.
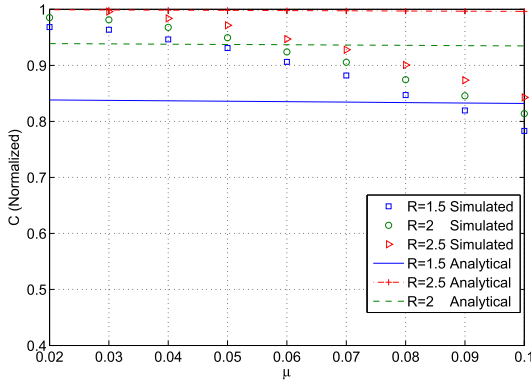
FIGURE 4. Clustering coefficient as a function of μ for different values of R. Network parameters that remain fixed are $A = 100$, $k_{global} = 5$, $\rho = 4$, $\xi = 3$ and $n_c = 1$.

FIGURE 5. Characteristic path length L as a function of μ for different values of R. Network parameters that remain fixed are $A = 100$, $k_{global} = 5$, $\rho = 4$, $\xi = 3$ and $n_c = 1$.
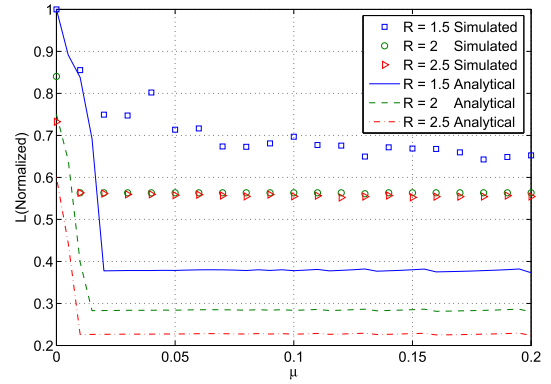
V. OBSERVATIONS

In this section, we describe the results of the analytical models of clustering coefficient C and characteristic path length L as we vary the length of local scale links R, and the scaling factor ξ. Both models, analytical and simulated, are evaluated in this section. Simulations are performed in Matlab, nodes are distributed according to a two-dimensional uniform random distribution with area A and density ρ. The Bellman-Ford algorithm was used for the calculation of shortest path. For the following evaluations we assumed a network of 400 nodes in an area of size $A = 100$ and $n_c = 1$. Unless stated otherwise, the default parameters of the network are $R = 2$, $\xi = 3$ and $k_{global} = 5$. The communication range of each node in each direction is modeled as a Gaussian random variable of mean R and standard deviation $0.2 \times R$. Fig. 4 plots the clustering coefficient of the network as functions of μ, for different values of R. The clustering coefficient C for the analytical model appears as a linearly decreasing function of μ with identical slopes, whereas in the simulation results the decrease in C is more sharp. The clustering coefficient has higher values for longer range R of local scale links for both, analytical model and simulation.

Moreover, it should be noted that the analytical model assumes that nodes are deployed in a circular shaped region, for mathematical tractability. The simulations make no such assumption. As a matter of fact, the deployment regions in the simulations are irregularly shaped, but are made to fit within a square region.

Fig. 5 plots the characteristic path length for various R. Higher values of R imply that destinations can be reached in fewer hops, thus reducing the characteristic path length. This is borne out by the curves of L. Moreover, a comparison of Fig. 4 and Fig. 5 clearly illustrates the phase difference in the reduction of C and L. This means the derived analytical model indeed captures the small world effect in the network. Unlike in Watts' β-model [4] of constructing small world networks, C lacks a sharp drop-off as $\mu \to 1$. The reason for this is the range limitation on shortcuts which imposes a degree of localization in a shortcut link's reach which leads
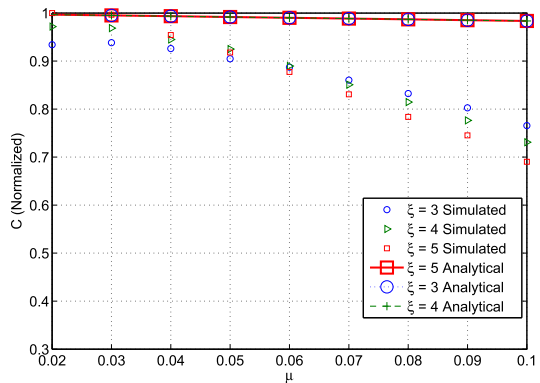

FIGURE 6. Clustering coefficient C as a function of μ for different ratios of global scale link to local scale link communication range ξ. Network parameters remain fixed at $A = 100$, $k_{global} = 5$, $\rho = 4$, $n_c = 1$ and $R = 1.5$.

to clustering. In addition, all construction methods of small world wireless network in section II add shortcuts on top of the existing geometric graph instead of rewiring existing links as the β-model does where each global scale link is added at the cost of removing a local scale link.

Fig. 6 and Fig. 7 plot clustering coefficient C and characteristic path length L as functions of μ for different values of global scale link scaling factors ξ. Recall that in deriving the analytical model for the clustering coefficient we made the assumption that $\xi \geq 2$, *i.e.*, shortcut links have a communication range of at least twice that of local scale links. Note that in Fig. 6, all plotted function of C overlap, *i.e.*, as long as as the assumption $\xi \geq 2$ holds, the clustering coefficient as a function of μ is independent of the global scaling factor ξ. The small world network effect is clearly visible by the large gap between clustering coefficient and characteristic path length. As expected, the drop in characteristic path length L drops off earlier as ξ increases, *i.e.* fewer shortcuts are necessary to achieve the same reduction in L as shortcuts get longer.

However, we observe that the small world effect consistently holds in two-dimensional spatial graphs even with
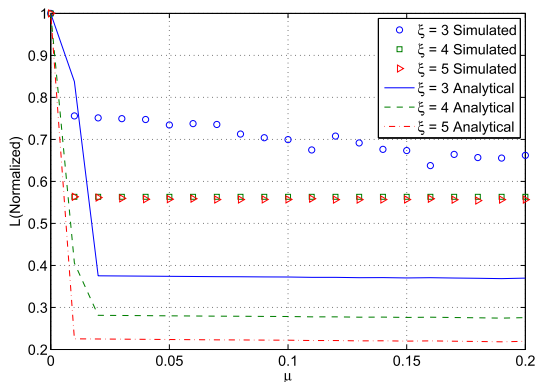
FIGURE 7. Characteristic path length *L* as a function of μ for different ratios of global scale link to local scale link communication range ξ. Network parameters remain fixed at $A = 100$, $k_{global} = 5$, $\rho = 4$, $n_c = 1$ and $R = 1.5$.

FIGURE 8. Graphical representation of integration term of *d* ($\Gamma(v)$).

range limited shortcuts such as those formed by wireless networks. What is also interesting is the fact that for sufficiently dense wireless networks the number of shortcuts that is needed to achieve a significant reduction in *L* is very small.

We concede that there are differences between the simulations and analytical results. We explain these differences by the following factors:

1) Several approximations that are used in the course of arriving at the analytical model. We attribute the mismatch to accumulated errors of approximation.

2) For mathematical tractability, the shape of the wireless network deployment region was assumed to be circular. In the simulations on the other hand, we assumed an approximately rectangular deployment region. This was done for reasons of simplicity, as well as to test the applicability of the conclusions drawn from the analytical model to arbitrarily shaped wireless network deployment regions.

VI. CONCLUSIONS

We derived analytical models for both clustering coefficient and characteristic path length of a two-dimensional spatial graph with range limited shortcuts that models the topological constraints to which D2D wireless networks are subject.

1) The model is sufficiently general to accommodate any small-world network construction methods in wireless networks previously proposed for wireless networks and is, to the authors' best knowledge, the first analytical model for networks with these constraints.

2) We observed that for sufficiently dense networks, characteristic path length can be reduced significantly by replacing a fraction $\mu \approx 1 - 5\%$ of the local scale nodes by global scale nodes providing shortcuts in the network. The order of μ, the fraction of nodes that are designated shortcut nodes, is about the same as the value of β, the rewiring probability, in Watts' small world network construction method.
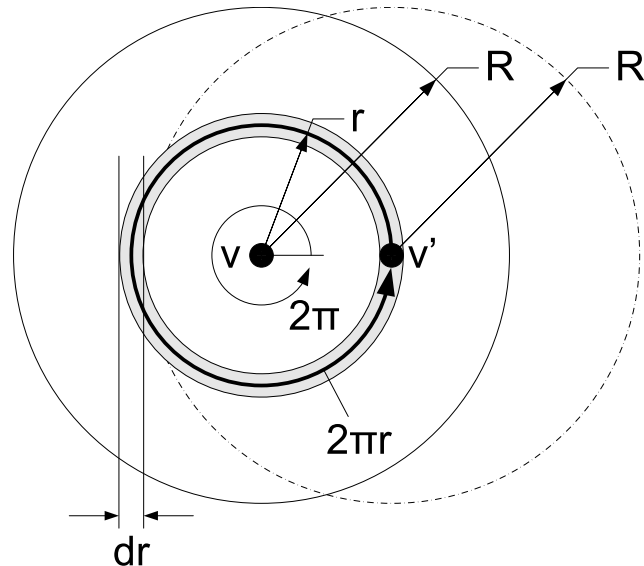
3) Whichever small world network construction method is applied carries with it a cost. The model lends itself for the task of designing wireless networks, *e.g.*, determining the number of shortcut nodes required to achieve a certain characteristic path length.

4) Although shortcut links added to a wireless network are range-limited, their addition to the topology still produces the small-world effect.

5) While the values of characteristic path length and clustering coefficient predicted by the analytical model differ significantly from those observed in simulations, the model remains accurate in predicting the presence of a small-world effect and the fraction of links μ that should constitute shortcuts.

Lemma 1: We derive the expression for $d(\Gamma(v))$, the number of links between the set of nodes consisting of v and all its neighbors $\Gamma(v)$. The region covered by $\Gamma(v)$ is approximated by a circular region of radius R centered at v. Consider another node v' at a distance r from node v shown in Fig. 8. Then the number of links from v' to other nodes in $\Gamma(v)$ is $\Delta(r)\rho'$. The narrow ring of width dr is inhabited by $2\pi r \rho'$ other nodes at the same distance r from v. The number of links from all nodes at distance r from v is $2\pi r \rho' \Delta(r)\rho'$. Then, to find $d((\Gamma(v))$, the total number of links between nodes v and $\Gamma(v)$, we integrate $2\pi r \rho' \Delta(r)\rho'$ with respect to r over $[0, R]$, the radius of communication of v.

$$d(\Gamma(v))$$
$$= \int_0^R \rho' 2\pi r \Delta(r)\rho' dr$$
$$= 4\pi R^2 \rho'^2 \int_0^R r \arccos \frac{r}{2R} dr - \frac{\pi}{2}\rho'^2 \int_0^R r^2 \sqrt{4R^2 - r^2} dr$$
$$= 4\pi R^2 \rho'^2 \cdot \mathcal{A}(R) - \frac{\pi}{2}\rho'^2 \cdot \mathcal{B}(R) \tag{A-1}$$

where $\mathcal{A}(R)$ and $\mathcal{B}(R)$ are evaluated in Equ. A-2 and Equ. A-3.

$$\mathcal{A}(R) = \left| \arcsin\left(\frac{r}{2R}\right)R^2 - \frac{1}{2}r\sqrt{1 - \frac{r^2}{4R^2}}R \right.$$

$$\left. + \frac{1}{2}r^2 \arccos\left(\frac{r}{2R}\right) \right|_0^R$$

$$= \frac{\pi}{3}R^2 - \frac{\sqrt{3}}{4}R \qquad \text{(A-2)}$$

$$\mathcal{B}(R) = \left| \frac{\frac{1}{3}r^3\sqrt{4R^2 - r^2}\,_2F_1\left(1.5; -0.5; 2.5; \frac{r^2}{4R^2}\right)}{\sqrt{1 - \frac{r^2}{4R^2}}} \right|_0^R \qquad \text{(A-3)}$$

$_2F_1(a; b, c, z)$ denotes the hypergeometric function (Equ. A-4) and is evaluated in Equ. A-5.

$$_2F_1(a; b; c; z) = \frac{\Gamma(c)}{\Gamma(b)\Gamma(c-b)} \int_0^1 \frac{t^{b-1}(1-t)^{c-b-1}}{(1-tz)^a}dt \qquad \text{(A-4)}$$

$$_2F_1\left(1.5; -0.5; 2.5; \frac{r^2}{4R^2}\right)$$

$$= \frac{\Gamma(2.5)}{\Gamma(-0.5)\Gamma(3)} \int_0^1 \frac{t^{-1.5}(1-t)^2}{\left(1 - \frac{r^2}{4R^2}t\right)^{1.5}}dt$$

$$= -0.1875 \int_0^1 \frac{t^{-1.5}(1-t)^2}{\left(1 - \frac{r^2}{4R^2}t\right)^{1.5}}dt \qquad \text{(A-5)}$$

Substituting the value of the hypergeometric function from Equ. A-5 into Equ. A-3 and produces Equ. A-6.

$$\mathcal{B}(R) = \frac{2}{3}R^4 \cdot_2 F_1(1.5; -0.5; 2.5; 0.25) - 0 = 0.6142 \cdot R^4 \qquad \text{(A-6)}$$

Substituting $\mathcal{A}(R)$ and $\mathcal{B}(R)$ from Equ. (A-2 and A-6) back into Equ. (A-1) gives Equ. (A-7).

$$d(\Gamma(v)) = 3.574\pi\rho'^2 R^4 - \sqrt{3}\pi\rho'^2 R^3 \qquad \text{(A-7)}$$

Lemma 2: We compute the area of region 3 in Fig. 3 for a node x distance from O denoted as $S(x)$, where $x > \sqrt{\frac{A_g}{\pi}}$. In order to proceed we compute the area of triangle BOJ denoted by $\Lambda(x)$. For $x > \sqrt{\frac{A_g}{\pi}}$, $\Lambda(x)$ can be expressed in previously defined terms as Equ. A-8.

$$\Lambda = \sqrt{\frac{A_g}{\pi}} \cdot \sqrt{\frac{A}{\pi}} \sin\beta \qquad \text{(A-8)}$$

Similarly, the area of sector JOJ' with central angle γ and radius $\sqrt{\frac{A}{\pi}}$ is denoted by $\widehat{\Lambda}(x)$. For $x > \sqrt{\frac{A_g}{\pi}}$, $\widehat{\Lambda}(x)$ can be expressed in previously defined terms as Equ. A-9.

$$\widehat{\Lambda}(x) = \frac{\gamma(x)}{2\pi}\pi\sqrt{\frac{A}{\pi}}^2 = \frac{A}{2\pi}(\pi - \alpha(x) - \beta) \qquad \text{(A-9)}$$

The area of sector BOB' with central angle $2\beta + \gamma$ and radius $\sqrt{\frac{A_g}{\pi}}$ is denoted by $\widehat{\widehat{\Lambda}}(x)$. For $x > \sqrt{\frac{A_g}{\pi}}$, $\widehat{\widehat{\Lambda}}(x)$ can be expressed as Equ. A-10.

$$\widehat{\widehat{\Lambda}}(x) = \frac{2\beta + \gamma(x)}{2\pi}\pi\sqrt{\frac{A_g}{\pi}}^2 = \frac{2\beta + \gamma(x)}{2\pi}A_g \qquad \text{(A-10)}$$

We now use $\Lambda(x)$, $\widehat{\Lambda}(x)$ and $\widehat{\widehat{\Lambda}}(x)$ to obtain the area of region 3 denoted by $S(x)$.

$$S(x) = 2\Lambda(x) + \widehat{\Lambda}(x) - \widehat{\widehat{\Lambda}}(x)$$

$$= \frac{2}{\pi}\sqrt{AA_g}\sin\beta + \frac{A}{2\pi}(\pi - \alpha(x) - \beta) - \frac{2\beta + \gamma(x)}{2\pi}A_g \qquad \text{(A-11)}$$

REFERENCES

[1] M. Penrose, *Random Geometric Graphs*. Oxford, U.K.: Oxford Univ. Press, 2003.

[2] W. Stallings, *Wireless Communications & Networks*. Upper Saddle River, NJ, USA: Prentice-Hall, 2004.

[3] I. F. Akyildiz, W. Su, Y. Sankarasubramaniam, and E. Cayirci, "Wireless sensor networks: A survey," *Comput. Netw.*, vol. 38, no. 4, pp. 393–422, 2002.

[4] D. J. Watts, *Small Worlds: The Dynamics of Networks Between Order and Randomness*. Princeton, NJ, USA: Princeton Univ. Press, 1999.

[5] B. Bollobás, *Random Graphs*. Cambridge, U.K.: Cambridge Univ. Press, 2001.

[6] G. Sharma and R. Mazumdar, "Hybrid sensor networks: A small world," in *Proc. 6th ACM Int. Symp. Mobile Ad Hoc Netw. Comput.*, New York, NY, USA, 2005, pp. 366–377.

[7] R. Chitradurga and A. Helmy, "Analysis of wired short cuts in wireless sensor networks," in *Proc. IEEE/ACS Int. Conf. Pervasive Services (ICPS)*, Jul. 2004, pp. 167–176.

[8] C.-Y. Wan, S. B. Eisenman, A. T. Campbell, and J. Crowcroft, "Siphon: Overload traffic management using multi-radio virtual sinks in sensor networks," in *Proc. 3rd Int. Conf. Embedded Netw. Sensor Syst.*, New York, NY, USA, 2005, pp. 116–129.

[9] M. U. Ilyas, M. Kim, and H. Radha, "Reducing packet losses in networks of commodity IEEE 802.15.4 sensor motes using cooperative communication and diversity combination," in *Proc. 28th IEEE Int. Conf. Comput. Commun. (INFOCOM)*, Rio de Janeiro, Brazil, Apr. 2009, pp. 1818–1826.

[10] D. L. Guidoni, R. A. F. Mini, and A. A. F. Loureiro, "On the design of resilient heterogeneous wireless sensor networks based on small world concepts," *Comput. Netw.*, vol. 54, no. 8, pp. 1266–1281, Jun. 2010. doi: 10.1016/j.comnet.2009.10.021.

[11] T. Jin, G. Noubir, and B. Sheng, "WiZi-cloud: Application-transparent dual ZigBee-WiFi radios for low power Internet access," in *Proc. IEEE NFOCOM*, Apr. 2011, pp. 1593–1601.

[12] Y. Zhang and Q. Li, "Howies: A holistic approach to ZigBee assisted WiFi energy savings in mobile devices," in *Proc. IEEE INFOCOM*, Apr. 2011, pp. 1366–1374.

[13] D. J. Watts, "Networks, dynamics, and the small-world phenomenon," *Amer. J. Sociol.*, vol. 105, no. 2, pp. 493–527, 1999.

[14] S. Milgram, "The small world problem," *Psychol. Today*, vol. 2, no. 1, pp. 60–67, 1967.

[15] P. Whoriskey, "Instant-messagers really are about six degrees from Kevin bacon," Washington Post, Washington, DC, USA, Tech. Rep., Aug. 2008. [Online]. Available: http://www.washingtonpost.com/wp-dyn/content/article/2008/08/01/AR2008080103718.html

[16] V. Latora and M. Marchiori, "Efficient behavior of small-world networks," *Phys. Rev. Lett.*, vol. 87, no. 19, pp. 198701-1–198701-4, 2001.

[17] J. M. Montoya and R. Solé, "Small world patterns in food Webs," *J. Theor. Biol.*, vol. 214, no. 3, pp. 405–412, 2002.

[18] C. Moore and M. E. J. Newman, "Epidemics and percolation in small-world networks," *Phys. Rev. E, Stat. Phys. Plasmas Fluids Relat. Interdiscip. Top.*, vol. 61, no. 5, pp. 5678–5682, 2000.

[19] C. Moore and M. E. J. Newman, "Exact solution of site and bond percolation on small-world networks," *Phys. Rev. E, Stat. Phys. Plasmas Fluids Relat. Interdiscip. Top.*, vol. 62, no. 5, pp. 7059–7064, 2000.

[20] V. Latora and M. Marchiori, "Is the Boston subway a small-world network?" *Phys. A, Stat. Mech. Appl.*, vol. 314, nos. 1–4, pp. 109–113, 2002.

[21] P. Sen, S. Dasgupta, A. Chatterjee, P. A. Sreeram, G. Mukherjee, and S. S. Manna, "Small-world properties of the Indian railway network," *Phys. Rev. E, Stat. Phys. Plasmas Fluids Relat. Interdiscip. Top.*, vol. 67, no. 3, 2003, Art. no. 36106.

[22] L. A. Adamic, "The small world Web," in *Research and Advanced Technology for Digital Libraries* (Lecture Notes in Computer Science). 1999, pp. 443–452.

[23] R. F. I. Cancho and R. V. Solé, "The small world of human language," *Proc. Roy. Soc. B, Biol. Sci.*, vol. 268, no. 1482, pp. 2261–2265, 2001.

[24] D. Cavalcanti, D. Agrawal, J. Kelner, and D. Sadok, "Exploiting the small-world effect to increase connectivity in wireless ad hoc networks," in *Proc. Int. Conf. Telecommun.*, 2004, pp. 388–393.

[25] R. A. Costa and J. Barros, "Dual radio networks: Capacity and connectivity," in *Proc. 5th Int. Symp. Modeling Optim. Mobile, Ad Hoc Wireless Netw. Workshops (WiOpt)*, 2007, pp. 1–6.

[26] J.-P. Hubaux, T. Gross, J.-Y. Le Boudec, and M. Vetterli, "Toward self-organized mobile ad hoc networks: The terminodes project," *IEEE Commun. Mag.*, vol. 39, no. 1, pp. 118–124, Jan. 2001.

[27] T. Dimitar, F. Sonja, M. Jani, and G. Aksenti, "Small world application layer for ad hoc networks," in *Proc. Telekomunikacioni Forum Telfor*, 2003, pp. 1–4.

[28] S. Dixit, E. Yanmaz, and O. K. Tonguz, "On the design of self-organized cellular wireless networks," *IEEE Commun. Mag.*, vol. 43, no. 7, pp. 86–93, Jul. 2005.

[29] A. Helmy. (2002). "Small large-scale wireless networks: Mobility-assisted resource discovery." [Online]. Available: https://arxiv.org/abs/cs/0207069

[30] A. Helmy, "Small worlds in wireless networks," *IEEE Commun. Lett.*, vol. 7, no. 10, pp. 490–492, Oct. 2003.

[31] M. E. J. Newman, C. Moore, and D. J. Watts, "Mean-field solution of the small-world network model," *Phys. Rev. Lett.*, vol. 84, no. 14, pp. 3201–3204, 2000.

[32] L. A. N. Amaral, A. Scala, M. Barthélémy, and H. E. tanley, "Classes of small-world networks," *Proc. Nat. Acad. Sci. USA*, vol. 97, no. 21, pp. 11149–11152, 2000.

[33] H. Inaltekin, M. Chiang, and H. V. Poor, "Average message delivery time for small-world networks in the continuum limit," *IEEE Trans. Inf. Theory*, vol. 56, no. 9, pp. 4447–4470, Sep. 2010. doi: 10.1109/TIT.2010.2054490.

[34] D. J. Watts and S. H. Strogatz, "Collective dynamics of 'small-world' networks," *Nature*, vol. 393, pp. 440–442, Jun. 1998.

[35] M. E. J. Newman and D. J. Watts, "Scaling and percolation in the small-world network model," *Phys. Rev. E, Stat. Phys. Plasmas Fluids Relat. Interdiscip. Top.*, vol. 60, no. 6, pp. 7332–7342, 1999.

[36] S. A. Pandit and R. E. Amritkar, "Characterization and control of small-world networks," *Phys. Rev. E, Stat. Phys. Plasmas Fluids Relat. Interdiscip. Top.*, vol. 60, no. 2, pp. 1119–1122, 1999.

[37] *Ansi/IEEE Part 15.4: Low Rate Wireless Personal Area Networks*, IEEE Standard 802.15.4.-2011, 2006.

[38] *Information Technology—Telecommunications and Information Exchange Between Systems—Local and Metropolitan Networks—Specific Requirements—Part 11: Wireless LAN Medium Access Control (MAC) and Physical Layer (PHY) Specifications: Higher Speed Physical Layer (PHY) Extension in the 2.4 GHz Band*, IEEE Starderd 802.11b-1999, 2003.

[39] M. U. Ilyas, M. Kim, and H. Radha, "On enabling cooperative communication and diversity combination in IEEE 802.15. 4 wireless networks using off-the-shelf sensor motes," *Wireless Netw.*, vol. 17, no. 5, pp. 1173–1189, 2011.

[40] D. G. Brennan, "Linear diversity combining techniques," *Proc. IEEE*, vol. 91, no. 2, pp. 331–356, Feb. 2003.

[41] R. Albert, H. Jeong, and A.-L. Barabási, "Error and attack tolerance of complex networks," *Nature*, vol. 406, no. 6794, pp. 378–382, 2000.

[42] C. Bettstetter, "On the minimum node degree and connectivity of a wireless multihop network," in *Proc. 3rd ACM Int. Symp. Mobile ad hoc Netw. Comput.*, 2002, pp. 80–91.

[43] C. Bettstetter and C. Hartmann, "Connectivity of wireless multihop networks in a shadow fading environment," *Wireless Netw.*, vol. 11, no. 5, pp. 571–579, Sep. 2005.

[44] L. Song and D. Hatzinakos, "Cooperative transmission in poisson distributed wireless sensor networks: Protocol and outage probability," *IEEE Trans. Wireless Commun.*, vol. 5, no. 10, pp. 2834–2843, Oct. 2006.

MUHAMMAD U. ILYAS received the B.E. degree (Hons.) in electrical engineering from the National University of Sciences and Technology, Rawalpindi, Pakistan, in 1999, the M.S. degree in computer engineering from the Lahore University of Management Sciences, Lahore, Pakistan, in 2004, and the M.S. and Ph.D. degrees in electrical engineering from Michigan State University, East Lansing, MI, USA, in 2009 and 2007, respectively.

He was a Postdoctoral Research Associate appointed jointly by the Electrical and Computer Engineering Department and the Computer Science and Engineering Department, Michigan State University. He worked under the joint supervision of Dr. H. Radha and Dr. A. Liu at East Lansing, MI, USA. He has been an Assistant Professor of computer science with the Faculty of Computing and Information Technology, University of Jeddah, Jeddah, Saudi Arabia, since 2016, and also has been an Assistant Professor of electrical engineering with the School of Electrical Engineering and Computer Science, National University of Sciences and Technology, Islamabad, Pakistan, since 2011.

MUHAMMAD MURTAZA KHAN received the B.Sc. degree (Hons.) in electrical engineering from the University of Engineering and Technology Taxila, Taxila, Pakistan, in 2000, the M.S. degree in computer software engineering from the National University of Sciences and Technology, EME College Rawalpindi, Pakistan, in 2005, and the M.S. and Ph.D. degrees in image processing from the Institut National Polytechnique de Grenoble, Grenoble, France, in 2006 and 2009, respectively.

From 2000 to 2004, he was a Software Engineer and later as a Senior Software Engineer with Streaming Networks Pvt., Ltd., Islamabad, where his responsibilities revolved around developing video drivers and implementation of optimized video codec solutions for Philips TriMedia processor. He has been an Assistant Professor of information technology with the Faculty of Computing and Information Technology, University of Jeddah, Jeddah, Saudi Arabia, since 2015, and also has been an Assistant Professor of Electrical Engineering with the School of Electrical Engineering and Computer Science, National University of Sciences and Technology, Islamabad, Pakistan, since 2010.

HAYDER RADHA received the B.S. degree (Hons.) in electrical engineering from Michigan State University, in 1984, the M.S. degree from Purdue University, in 1986, and the Ph.M. and Ph.D. degrees from Columbia University, in 1991 and 1993, respectively. From 1996 to 2000, he was with Philips Research, where he was a Principal Member of Research Staff and then as a Consulting Scientist with the Video Communications Research Department. He was a Member of Technical Staff at Bell Laboratories, where he worked, from 1986 to 1996, in digital communications, image processing, and broadband multimedia. He is currently a Professor of electrical and computer engineering with Michigan State University, the Associate Chair for Research of the ECE Department, and the Director of the Wireless and Video Communications Laboratory.

AHMED AL-GHAMDI graduated from the Department of Electrical Engineering and Computer Science, School of Engineering, The Catholic University of America, Washington, D.C., USA, with an emphasis in network security. He received the M.Sc. degree in information system from DePaul University, Chicago, in 2010. He is currently an Assistant Professor with the College of Computer Science and Engineering, University of Jeddah, Jeddah, Saudi Arabia.

He practiced IT for over six years. He started his technical career as a Platform Specialist and eventually became a Network Administrator at Batelco Jeraisy Ltd. (Atheer), in 2003. He then practiced teaching at the Royal Commission, Yanbu, for two Years before he became an IT Manager at Al Musahim Gate Company, in 2006.

ASMAA MUNSHI received the B.Sc. degree in computer science from King Abdulaziz University, Jeddah, Saudi Arabia, in 2004, and the master's degree (Hons.) in internet security and forensics and the Ph.D. degree in information system (information security) from Curtin University, Australia, in 2009 2014, respectively. She is currently an Assistant Professor of cybersecurity with the College of Computer Science and Engineering, University of Jeddah, Jeddah, Saudi Arabia. She is also serving as the Supervisor of the Department of Cybersecurity, University of Jeddah, Saudi Arabia. Her research interests include educational technology, e-learning, and information security.

• • •